

Detecting and Ranking Causal Anomalies in End-to-End Complex System

Ching Chang

Wen-Chih Peng

National Chiao Tung University, Hsinchu, Taiwan
{blacksnail789521.cs05g, wcpeng}@nctu.edu.tw

Abstract

With the rapid development of technology, the automated monitoring systems of large-scale factories are becoming more and more important. By collecting a large amount of machine sensor data, we can have many ways to find anomalies. We believe that the real core value of an automated monitoring system is to identify and track the cause of the problem. The most famous method for finding causal anomalies is RCA [1], but there are many problems that cannot be ignored. They used the AutoRegressive eXogenous (ARX) model to create a time-invariant correlation network as a machine profile, and then use this profile to track the causal anomalies by means of a method called fault propagation. There are two major problems in describing the behavior of a machine by using the correlation network established by ARX: (1) It does not take into account the diversity of states (2) It does not separately consider the correlations with different time-lag. Based on these problems, we propose a framework called *Ranking Causal Anomalies in End-to-End System* (RCAE2E), which completely solves the problems mentioned above. In the experimental part, we use synthetic data and real-world large-scale photoelectric factory data to verify the correctness and existence of our method hypothesis.

1 Introduction

Nowadays, in order to achieve an automated surveillance system, large-scale factories are equipped with multiple sensors. With an automated surveillance system, it is easier to monitor the execution status of each machine. In the past, many people have done the automatic detection of complex machine anomalies. Gertler et al. [2] proposed using each sensor's respective behavior to suggest various restrictions, and if it exceeds that condition, there will be a warning. However, if each sensor is considered separately, the correlations between different sensors will not be considered. Therefore, today's methods [3] tend to create a profile for the system to preserve the information of the correlations. The correlation network is one of the most famous methods used

to express machine profiles [3]. In the correlation network, a node represents a sensor and an edge stands for a correlation between two sensors. If there is a strong correlation between the two sensors, it means that data from these two sensors have a strong direct relationship. In Ge et al. [4] and Tao et al. [5]'s respective proposed methods, both used these correlations to detect anomalous nodes. They observed the percentage of broken edges (correlations) to determine whether the node is anomalous. The obvious disadvantage of these methods is that it did not take into account the nature of fault propagation. In the method proposed by Cheng et al. [1], called *Ranking Causal Anomalies* (RCA), they fully considered the situation of fault propagation. They claimed that because there are few cases in which the system errors are isolated, it's unlikely that the nodes around the anomalous node are not affected. If there is a node becomes anomalous, then the nodes that have strong correlations with that anomalous node will be affected in succession. Because of this, all the anomalies they found will be the source of anomalies.

However, RCA [1] has two major drawbacks. The first major drawback in RCA is that they used a single time-invariant model to describe the behavior of a machine, which means they assumed the behavior of the machine will not change from beginning to end. We have raised a strong suspicion about this view because most real-world machines cannot be measured by a single time-invariant model. Instead of building a correlation network for each machine, we believe that we need to build a correlation network for each state of the machine. The second major drawback in RCA is that they did not separately consider the correlations with different time-lag. Although the correlation network established using the ARX model can contain the correlations with different time-lag, we have no way to consider these correlations separately. We believe that separately considering the correlations with different time-lag can simulate fault propagation more accurately.

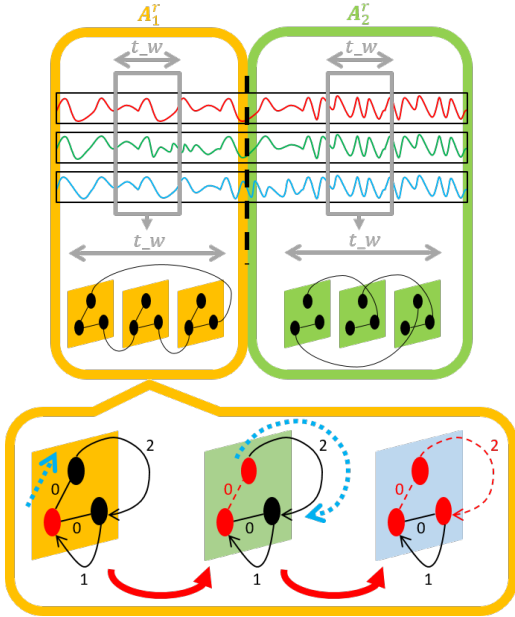


Figure 1: RCAE2E includes two core methods. The first is TICC_GTC for profile creation (upper half of the figure), and the second is RCA_SCC for ranking causal anomalies (bottom half of the figure).

In order to solve the two major drawbacks of RCA, we propose a method to create a profile called Toeplitz Inverse Covariance-based Clustering with Global Temporal Consistency (TICC_GTC), which is derived from Hallac et al.’s method [6]. Their proposed method, Toeplitz Inverse Covariance-based Clustering (TICC), can simultaneously perform segmentation and clustering on multivariate time series data. We can use TICC’s segmentation to solve the problem that RCA does not consider the diversity of states. We can also use TICC’s clustering to solve the problem that RCA does not separately consider the correlations with different time-lag. The only difference between our proposed TICC_GTC and TICC is that we have added a new constraint called global temporal consistency. For the application of large-scale factory machine, we believe that the cluster assignments of adjacent runs should be aligned because the behavior of factory production is basically very regular. So, we can use the global temporal consistency to encourage two data points, which have the same timestamp and adjacent run number, to have the same cluster assignment. After generating the profile by TICC_GTC, we use our proposed method Ranking Causal Anomalies with Separate Consideration of the Correlations with different time-lag (RCA_SCC) to find the causal anomalies. As the name implies, RCA_SCC is the version of RCA that separately considers the correlations with different time-lag.

In conclusion, based on the limitations of current methods, we propose a causal anomaly detection algorithm for the factory machine, which we call *Ranking Causal Anomalies in End-to-End System* (RCAE2E). Figure 1 is a schematic diagram of RCAE2E. Our contributions can be summarized as follows.

1. We propose RCAE2E (a framework that can directly look for causal anomalies in end-to-end system). We completely solve the problem of not considering the diversity of states and not separately considering the correlations with different time-lag in RCA.
2. We propose TICC_GTC (a method to build a profile). We add global temporal consistency on TICC to make it more suitable for factory machine applications.
3. We propose RCA_SCC (a method to find causal anomalies). We separately consider the correlations with different time-lag when looking for causal anomalies.

2 preliminaries and problem definition

In this section, we first introduce two methods that are most relevant to this paper: Ranking Causal Anomalies (RCA) [1] and Toeplitz Inverse Covariance-based Clustering (TICC) [6]. In the end, we will describe the problem definition for this paper.

2.1 Ranking Causal Anomalies (RCA) The purpose of RCA is to find causal anomalies in the correlation network. First, they used the historical data to find the correlation network in the training state. (Here they used the ARX model to build it.) And then in the testing state, they checked if the new incoming data will also have these correlations in the correlation network. If the correlation disappears, it means that the two sensors connecting through this correlation are likely to have some problems. Therefore, they used vanishing correlations to reconstruct propagated anomaly scores (called *Reconstruction Error*), and used the label propagation technique [7] to determinate the source of the anomalies (called *Fault Propagation*). We will introduce these two concepts of RCA.

2.1.1 Fault Propagation There is a major assumption in RCA that system faults are rarely isolated. They thought that when a node has a problem, that problem will propagate to the nearby nodes. And the propagation path will be the correlations between the nodes. They used two vectors to describe this propagation process. The first one is causal anomaly score vector

Table 1: Notations

Symbol	Definition	Dimension
$\mathbf{x}^{t,r}$	the data subsequence at time $t - (t.w - 1)$ to time t , run r	$\mathbb{R}^{N \times t.w}$
$T(R)$	the length of single run data (the number of run data)	\mathbb{R}
N	the number of sensors	\mathbb{R}
$t.w$ ($r.w$)	the window size of multiple data points (multiple run data)	\mathbb{R}
K	the number of clusters in TICC_GTC	\mathbb{R}
λ, β, α (c, ξ)	the parameters in TICC_GTC (RCA_SCC)	\mathbb{R}
\mathbf{A}_k^r	the adjacency matrix of MRF for cluster k from run $r - (r.w - 1)$ to run r	$\mathbb{R}^{(N \cdot t.w) \times (N \cdot t.w)}$
\mathbf{b}^t	the propagated anomaly score vector at time t	$\mathbb{R}^{N \times 1}$
\mathbf{s}^t	the causal anomaly score vector at time t	$\mathbb{R}^{N \times 1}$
\mathbf{A}^t (\mathbf{B}^t)	the adjacency matrix of (broken) MRF from time $t - (t.w - 1)$ to time t	$\mathbb{R}^{(N \cdot t.w) \times (N \cdot t.w)}$
$\mathbf{A}^{t, (time_lag)}$ ($\mathbf{B}^{t, (time_lag)}$)	the (broken) correlation network from time τ to time $\tau + time_lag$ ($t - (t.w - 1) \leq \tau \leq t - time_lag$)	$\mathbb{R}^{N \times N}$

(\mathbf{s}), which represents whether each sensor is a casual anomaly. The second one is propagated anomaly score vector (\mathbf{b}), which records the anomalous system status of each sensor after fault propagation. The entire propagation process from \mathbf{s} to \mathbf{b} can be described by the following optimization problem

$$(2.1) \quad \min_{\mathbf{b} \geq 0} c \sum_{i,j=1}^N A_{ij} \underbrace{\left\| \frac{b_i}{\sqrt{D_{ii}}} - \frac{b_j}{\sqrt{D_{jj}}} \right\|^2}_{\text{smoothness constraint}} + (1-c) \sum_{i=1}^N \underbrace{\|b_i - s_i\|^2}_{\text{fitting constraint}}.$$

There are two main parts inside this objective function. The first part is *smoothness constraint*, which means that they hoped the node's anomalous system status would be similar to its nearby nodes. The second part is *fitting constraint*, meaning that they hoped the final state of the entire system would be similar to the initial state.

2.1.2 Reconstruction Error The idea of reconstruction error is to use propagated anomaly score vector \mathbf{b} to reconstruct the broken network. We mentioned earlier that they created a corresponding broken network for each new incoming data in the testing state. The broken network is used to record the broken correlations between two sensors. A broken correlation means that at least one of these two sensors connected by this edge is anomalous. Therefore, the product of the two sensors' propagated anomaly score must be large. And because a large value of an edge in the broken network represents a broken correlation, we can use the product of the two sensors' propagated anomaly score to approximate the values in the broken network. The objective

function of reconstruction error is

$$(2.2) \quad \arg \min_{\mathbf{b} \geq 0} \sum_{i,j=1}^N (b_i \cdot b_j \cdot M_{ij} - \tilde{B}_{ij})^2.$$

2.2 Toeplitz Inverse Covariance-based Clustering (TICC) The purpose of TICC is to segment multivariate time series data into multiple interpretable states or clusters. In TICC, each cluster is a correlation network described by Markov Random Field (MRF). MRF can have many layers, which means that the correlation network can contain the correlations with different time-lag. The number of MRF's layers equals to the window size, which is a time interval representing the number of time points we need to consider at one timestamp. They learned each MRF based on the calculation of the sparse Gaussian inverse covariance matrix [8], and each MRF can be represented by a adjacency matrix \mathbf{A} [9]. When $A_{i,j}$ is large, it means that the partial correlation between sensor i and sensor j is very strong. Now, in order to represent the entire cluster with an single MRF, they added the block Toeplitz constraint [10] into graphical lasso. Therefore, it is guaranteed that any edge between layer i and layer $i + t$ will also exist in layer $i + k$ and layer $i + k + t$. It means that in this cluster, we can use this MRF to describe all the data subsequences. The output of TICC is the profile of multivariate time series data, which includes the MRFs ($\mathbf{A} = \{\mathbf{A}_k : 1 \leq k \leq K\}$) representing each cluster and the cluster assignments ($\mathbf{P} = \{\mathbf{P}_k : 1 \leq k \leq K\}$) of each data subsequence. The overall optimization problem of

TICC is

$$(2.3) \quad \arg \min_{\mathbf{A} \in \mathbf{T}, \mathbf{P}} \sum_{k=1}^K \left[\underbrace{\|\lambda \circ \mathbf{A}_k\|_1}_{\text{sparsity}} + \sum_{\mathbf{x}^t \in \mathbf{P}_k} \left(\underbrace{-\ell\ell(\mathbf{x}^t, \mathbf{A}_k)}_{\text{log likelihood}} + \underbrace{\beta \mathbb{1}\{\mathbf{x}^{t-1} \notin \mathbf{P}_k\}}_{\text{temporal consistency}} \right) \right].$$

$\mathbf{A} \in \mathbf{T}$ means the MRF we found must have the block Toeplitz structure. There are three main parts inside this objective function. The first part is *sparsity*, which means that they hoped the MRFs can be very sparse. Based on past experience, we know that sparse graphical representations are a very effective way to avoid overfitting [11]. The second part is *log likelihood*, which means the likelihood that data subsequence \mathbf{x}^t comes from cluster i . The equation for log likelihood is

$$(2.4) \quad \ell\ell(\mathbf{x}^t, \mathbf{A}_k) = -\frac{1}{2}(\mathbf{x}^t - \mu_k)^T \mathbf{A}_k (\mathbf{x}^t - \mu_k) + \frac{1}{2} \log \det \mathbf{A}_k - \frac{n}{2} \log(2\pi).$$

The third part is *temporal consistency*, which means that they wanted the cluster assignments of two adjacent data subsequences to be the same. If the cluster assignment of current data subsequence is not the same as the previous data subsequence, there will be a penalty.

2.3 Problem Definition The input data of RCAE2E is multivariate time series data with multiple runs. We use \mathbf{X} to indicate input data: $\mathbf{X} = \{x_n^{t,r} : 1 \leq n \leq N, 1 \leq t \leq T, 1 \leq r \leq R\}$, where N is the number of sensors, T is the length of single run data, and R is the number of run data. However, when analyzing the input data, we do not look at each timestamp individually. Instead, we look at a short subsequence, which window size is $t_w \ll \mathbf{T}$. The reason is that when we establish the behavior of the machine, we must consider the context of the data we analyzed. As a result, we can have more understanding of the data. The output data of RCAE2E is the causal anomaly score for each sensor of each data point in the anomalous run data, and the higher value means the more likely this sensor is a causal anomaly. We use \mathbf{Y} to indicate output data: $\mathbf{Y} = \{s_n^t : 1 \leq n \leq N, 1 \leq t \leq T\}$.

3 Framework of RCAE2E

In this section, we present the framework of RCAE2E. We use a flowchart (Figure 2) to describe the framework so that the whole process can be better understood. All notations can be found in Table 1.

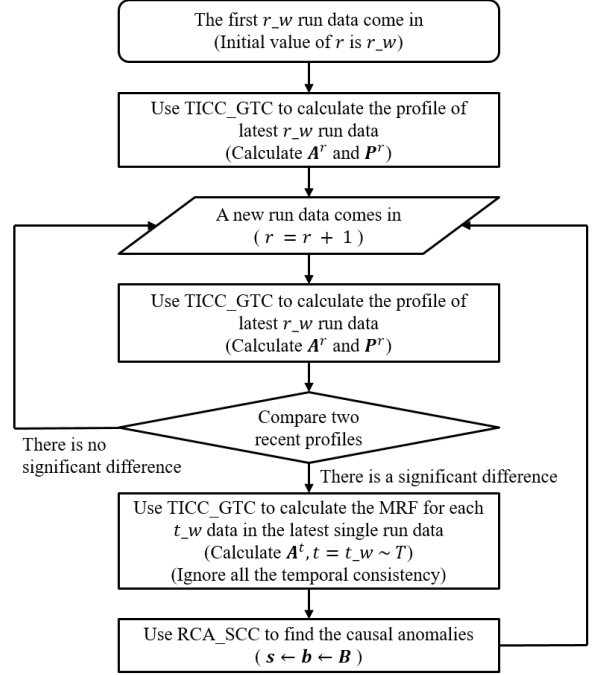


Figure 2: Flowchart of RCAE2E

At the beginning of the execution of RCAE2E, we need to have r_w run data. r is the index used to record the run number of the latest run data, and we can get $\mathbf{A}^r = \{\mathbf{A}_k^r : 1 \leq k \leq K\}$ and $\mathbf{P}^r = \{\mathbf{P}_k^r : 1 \leq k \leq K\}$ every time we use TICC_GTC to calculate the profile of r_w run data. Whenever there is a new run data coming in, we will do three things: (1) r plus 1. (2) Mark the last calculated profile as old profile. (3) Calculate the profile of the latest r_w run data and mark it as the new profile. When we have more than one profile (i.e. both new profile and old profile have values.), we can enter the profiles comparison. We can use the comparison of two latest profiles to determine if the latest run data is abnormal. This is because if the latest run data has some severe anomalies, it will cause the latest profile to be significantly different from the previous profile. If we find the anomalous run data, we will move on to the next stage: looking for the causal anomalies. We feed this anomalous run data into TICC_GTC to create the MRF of each data subsequence and then compare these MRFs with the ground truth MRFs to get the broken MRF for each data subsequence. It should be noted that when using TICC_GTC to create the MRF of each data subsequence in the anomalous run data, we ignore the local temporal consistency because we need to find the MRF that can represent each data subsequence. (There is no global temporal consistency because there is only one run data.) Finally, we feed the ground truth MRF

and the broken MRF of each data subsequence into the RCA_SCC, and we can get the causal anomaly score vector for each data point (not the data subsequence).

4 Detailed Methods of RCAE2E

In this section, we will introduce three detailed methods included in RCAE2E, which are TICC_GTC, Compare Two Profiles, and RCA_SCC.

4.1 TICC_GTC Traditionally, when analyzing multiple run data, we serially connect multiple run data into a long time series data, and then directly feed them into the model for analysis. We think that this method is not good because this will not take into account the state stability between adjacent run data. In general, the behavior of factory production is very regular, so the state distribution of adjacent run should be very similar. We need to encourage two data subsequences, which have the same timestamp and adjacent run number, to have the same cluster assignment. We call this new constraint *global temporal consistency* (GTC), and renamed the original temporal consistency in TICC to *local temporal consistency*.

TICC_GTC is TICC plus GTC, so the original objective function of TICC (Problem (2.3)) will become to

$$(4.5) \quad \arg \min_{\mathbf{A}^r \in \mathbf{T}, \mathbf{P}^r} \sum_{k=1}^K \left[\underbrace{\|\lambda \circ \mathbf{A}_k^r\|_1}_{\text{local temporal consistency}} + \sum_{\mathbf{x}^{t^r} \in \mathbf{P}_k^r} \left(\underbrace{-\ell(\mathbf{x}^{t^r}, \mathbf{A}_k^r)}_{\text{global temporal consistency}} \right) + \beta \mathbb{1}\{\mathbf{x}^{[t-1]^r} \notin \mathbf{P}_k^r\} + \alpha \mathbb{1}\{\mathbf{x}^{t^{r-1}} \notin \mathbf{P}_k^r\} \right].$$

We can solve Problem (4.5) by using a variation of Expectation Maximization (EM) algorithm, which alternates between assigning data subsequences to clusters and updating the MRFs. Because the only thing related to temporal consistency is assigning data subsequences to clusters (we will fix \mathbf{A}^r), we can change Problem (4.5) to

$$(4.6) \quad \arg \min_{\mathbf{P}^r} \sum_{k=1}^K \sum_{\mathbf{x}^{t^r} \in \mathbf{P}_k^r} \left(-\ell(\mathbf{x}^{t^r}, \mathbf{A}_k^r) + \beta \mathbb{1}\{\mathbf{x}^{[t-1]^r} \notin \mathbf{P}_k^r\} + \alpha \mathbb{1}\{\mathbf{x}^{t^{r-1}} \notin \mathbf{P}_k^r\} \right).$$

In Figure 3, the node represents the negative log likelihood of the data subsequence being assigned to the corresponding cluster, and the edge represents the

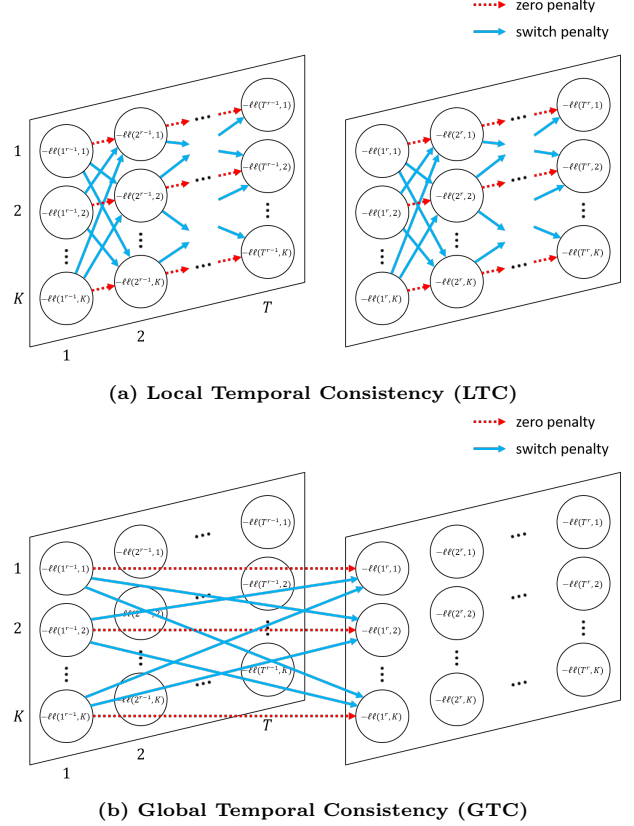


Figure 3: Temporal Consistency

cost when switching the cluster assignment. We need to choose a minimum-cost path from time 1 to time T in each run, so there are r_w paths in total. We use dynamic programming (Algorithm 1) to solve Problem (4.6). In Algorithm 1, for each timestamp, we use the Cartesian product to enumerate all combinations of each run selecting one cluster (use AllComb to store), and then find the best solution so far for each combination. We can find the solution by solving Problem (4.7), which can be formulated as follows:

$$(4.7) \quad \text{CurrCost}[\text{CurrIdx}] = \min(\text{PrevCost}[\text{PrevIdx}] - \ell(t^r, k) + \text{switch penalty}),$$

where the switch penalty includes LTC and GTC. The time complexity of Algorithm 1 is $O(K^{r_w^2} \cdot r_w \cdot T)$. Algorithm 2 is the pseudo code of Problem (4.7), with lines 2 ~ 6 representing LTC and lines 7 ~ 11 representing GTC.

4.2 Compare Two Profiles When comparing two profiles, we need to do two things. First, we need to reduce the length of both profiles to length T because

Algorithm 1: Assign Data Subsequences to Clusters

```
1 given  $\beta > 0, \alpha > 0, -\ell(t^r, k)$ .
2 AllComb = list of all combinations of each run
  selecting one cluster.
  (length of AllComb =  $K^{r \cdot w}$ ).
3 PrevCost = list of length(AllComb) zeros.
4 CurrCost = list of length(AllComb) infinite.
5 PrevPath = list of length(AllComb) empty
  lists.
6 CurrPath = list of length(AllComb) empty
  lists.
7 for  $t = 1, \dots, T$  do
8   CurrCost = list of length(AllComb) infinite.
9   for CurrIdx = 1, ..., length(AllComb) do
10    for PrevIdx = 1, ..., length(AllComb)
11     do
12      CurrCostPlusPrevCost = CalCost().
13      if CurrCostPlusPrevCost <
14       CurrCost[CurrIdx] then
15        CurrCost[CurrIdx] =
16        CurrCostPlusPrevCost.
17        CurrPath[CurrIdx] =
18        PrevPath[PrevIdx]
19        .append(AllComb[CurrIdx]).
20     end
21    end
22   end
23   PrevCost = CurrCost.
24   PrevPath = CurrPath.
25 end
26 FinalMinIdx = index of minimum value of
  CurrCost.
27 FinalCost = CurrCost[FinalMinIdx].
28 FinalPath = CurrPath[FinalMinIdx].
29 return FinalCost, FinalPath.
```

Algorithm 2: CalCost

```
1 CurrCostPlusPrevCost = PrevCost[PrevIdx]
   $-\ell(t^r, k)$  corresponding to AllComb[CurrIdx].
2 for  $r = 1, \dots, r \cdot w$  do
3   if  $t \neq 0$  and AllComb[PrevIdx][ $r$ ]  $\neq$ 
4   AllComb[CurrIdx][ $r$ ] then
5     CurrCostPlusPrevCost +=  $\beta$ .
6   end
7 end
8 for  $r = 1, \dots, r \cdot w$  do
9   if  $r \neq 0$  and AllComb[PrevIdx][ $r$ ]  $\neq$ 
10  AllComb[CurrIdx][ $r$ ] then
11    CurrCostPlusPrevCost +=  $\alpha$ .
12  end
13 end
14 return CurrCostPlusPrevCost.
```

the current profile length is $T \times r \cdot w$. The reason is that at each timestamp, we want to find an MRF that can represent the data subsequences of all run data. So, the method of reducing the length is to average the MRFs with the same timestamp. (There are $r \cdot w$ MRFs at each timestamp.) Second, we need to calculate the difference score for these two averaged profiles. We first calculate the cosine distance ($1 - \text{cosine similarity}$) of the two corresponding MRFs at each timestamp and then average the cosine distances of all timestamps.

4.3 RCA_SCC When we compare two profiles and find that there are significant differences, we will enter the stage of finding causal anomalies. We feed this anomalous run data into TICC-GTC to create the MRF of each data subsequence and then compare these MRFs with the ground truth MRFs to get the broken MRF for each data subsequence. Finally, we feed the ground truth MRF and the broken MRF of each data subsequence into RCA_SCC. The difference between RCA_SCC and RCA is that the MRFs we feed into RCA_SCC can contain the correlations with different time-lag. Next We will introduce three parts of RCA_SCC: *Convert from RCA to RCA_SCC*, *Get the s of Each Data Subsequence* and *Get the s of Each Data Point*.

4.3.1 Convert from RCA to RCA_SCC In order to simplify the formula, we first convert the two objective functions (*Fault Propagation* and *Reconstruction Error*) in the RCA into vector form. Problem (2.1) can be converted into the following formula:

$$(4.8) \quad \min_{\mathbf{b} \geq \mathbf{0}} c\mathbf{b}^T(\mathbf{I}_{N \cdot t \cdot w} - \tilde{\mathbf{A}})\mathbf{b} + (1 - c)\|\mathbf{b} - \mathbf{s}\|_F^2,$$

and Problem (2.2) can be converted into the following formula:

$$(4.9) \quad \arg \min_{\mathbf{b} \geq 0} \|(\mathbf{b}\mathbf{b}^T) \circ \mathbf{M} - \widetilde{\mathbf{B}}\|_F^2.$$

Next, we need to turn Problem (4.8) and Problem (4.9) into the format of RCA_SCC. The conversion of RCA to RCA_SCC requires two steps: expand the dimension and convert to the correct time representation. The rules of converting RCA to RCA_SCC can be referred to Figure 4. Because the MRF considered by RCA_SCC can contain correlations with different time-lag, the dimension of \mathbf{A} we use in RCA_SCC is t_w times larger than the \mathbf{A} we used in RCA ($\mathbb{R}^{N \times N}$ becomes $\mathbb{R}^{(N \cdot t_w) \times (N \cdot t_w)}$). Also, we must expand the dimension corresponding variables, such as \mathbf{B} , \mathbf{b} , \mathbf{s} , by t_w times. However, it is not enough to simply expand the dimension, because now we just think of t_w consecutive data points as having the same timestamp. So after expanding the dimension, we need to convert these $N \cdot t_w$ sensors into N sensors of t_w consecutive timestamps. Based on the above rules, we can get the objective function of RCA_SCC's *Fault Propagation* by converting Problem (4.8) into the following formula:

$$(4.10) \quad \min_{\mathbf{b}^{t-(t_w-1) \sim t} \geq 0} c(\mathbf{b}^{t-(t_w-1) \sim t})^T (\mathbf{I}_{N \cdot t_w} - \widetilde{\mathbf{A}}^t) \mathbf{b}^{t-(t_w-1) \sim t} + (1-c) \|\mathbf{b}^{t-(t_w-1) \sim t} - \mathbf{s}^{t-(t_w-1) \sim t}\|_F^2.$$

Also, we can get the objective function of RCA_SCC's *Reconstruction Error* by converting Problem (4.9) into the following formula:

$$(4.11) \quad \arg \min_{\mathbf{b}^{t-(t_w-1) \sim t} \geq 0} \|[\mathbf{b}^{t-(t_w-1) \sim t} (\mathbf{b}^{t-(t_w-1) \sim t})^T] \circ \mathbf{M}^t - \widetilde{\mathbf{B}}^t\|_F^2.$$

4.3.2 Get the \mathbf{s} of Each Data Subsequence We are now going to solve the two objective functions of RCA_SCC (Problem (4.10) and Problem (4.11), respectively). Solving the objective function of RCA_SCC's *Fault Propagation* (Problem (4.10)) is very simple, we can directly differentiate with respect to $\mathbf{b}^{t-(t_w-1) \sim t}$ to get the closed-form solution. So the closed-form solution of Problem (4.10) is [7]

$$(4.12) \quad \mathbf{b}^{t-(t_w-1) \sim t} = \mathbf{E}^t \mathbf{s}^{t-(t_w-1) \sim t},$$

where

$$(4.13) \quad \mathbf{E}^t = (1-c)(\mathbf{I}_{N \cdot t_w} - c\widetilde{\mathbf{A}}^t)^{-1}.$$

After getting Equation (4.12), we can replace $\mathbf{b}^{t-(t_w-1) \sim t}$ in the objective function (Problem (4.11))

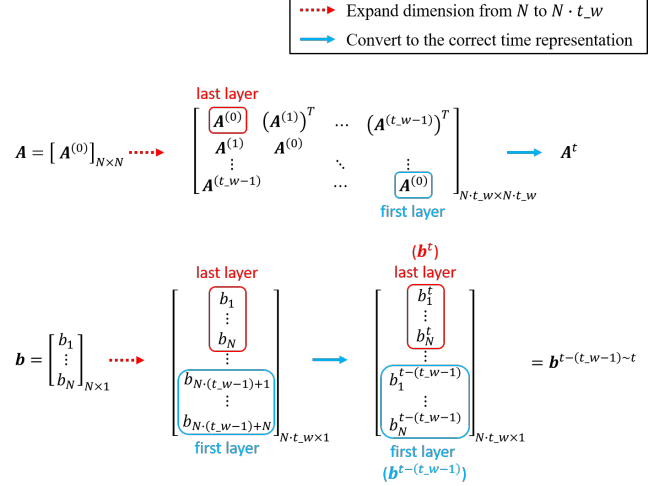


Figure 4: Convert from RCA to RCA_SCC

of RCA_SCC's *Reconstruction Error* with $\mathbf{s}^{t-(t_w-1) \sim t}$. In addition, because the number of root cause anomalies are usually not very large in the system, we added L1 norm to $\mathbf{s}^{t-(t_w-1) \sim t}$ to control the number of root cause anomalies we found. So, Problem (4.11) can be converted into the following formula:

$$(4.14) \quad \arg \min_{\mathbf{s}^{t-(t_w-1) \sim t} \geq 0} \|[\mathbf{E}^t \mathbf{s}^{t-(t_w-1) \sim t} (\mathbf{s}^{t-(t_w-1) \sim t})^T (\mathbf{E}^t)^T] \circ \mathbf{M}^t - \widetilde{\mathbf{B}}^t\|_F^2 + \xi \|\mathbf{s}^{t-(t_w-1) \sim t}\|_1.$$

We use an iterative multiplicative updating algorithm to solve Problem (4.14) [1]. The updating rule is Equation (4.15). We can guarantee that if we use Equation (4.15) to update the Problem (4.14), each update will monotonically decrease the value of the objective function. The time complexity of Equation (4.15) is $O(Iter \cdot (N \cdot t_w)^3)$, where *Iter* represents the number of updates to convergence. Due to space limitation, we omit the derivation of Equation (4.15) and the proof of its convergence. The relevant derivation and proof can refer to [1].

4.3.3 Get the \mathbf{s} of Each Data Point It should be noted that the $\mathbf{s}^{t-(t_w-1) \sim t}$ calculated from Problem (4.14) corresponds to each data subsequence, not each data point. In other words, for each sliding window, the $\mathbf{s}^{t-(t_w-1) \sim t}$ we calculated contains t_w data points. What we ultimately ask is the \mathbf{s}^t of each data point, not the $\mathbf{s}^{t-(t_w-1) \sim t}$ of each data subsequence. So we have to split the calculated $\mathbf{s}^{t-(t_w-1) \sim t}$ into t_w \mathbf{s}^t . Because of this, each data point will correspond to multiple \mathbf{s}^t . (Because the distance that each time the sliding window moves is one timestamp.) Therefore, the final \mathbf{s}^t of each

(4.15)

$$\mathbf{s}^{t-(t-w-1)\sim t} = \mathbf{s}^{t-(t-w-1)\sim t} \circ \left(\frac{4\{[(\mathbf{E}^t)^T \widetilde{\mathbf{B}}^t] \circ \mathbf{M}^t\} \mathbf{E}^t \mathbf{s}^{t-(t-w-1)\sim t}}{4\{[(\mathbf{E}^t)^T \mathbf{E}^t \mathbf{s}^{t-(t-w-1)\sim t} (\mathbf{s}^{t-(t-w-1)\sim t})^T (\mathbf{E}^t)^T] \circ \mathbf{M}^t\} \mathbf{E}^t \mathbf{s}^{t-(t-w-1)\sim t} + \xi \mathbf{1}_{N \cdot t-w}} \right)^{\frac{1}{4}}$$

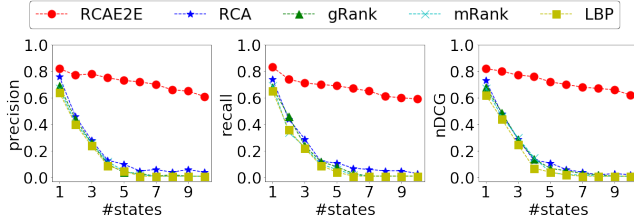


Figure 5: Performance vs. #states

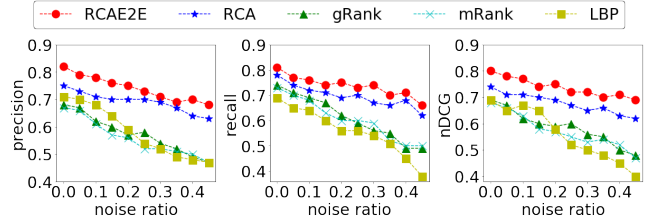


Figure 7: Performance vs. Noise Ratio

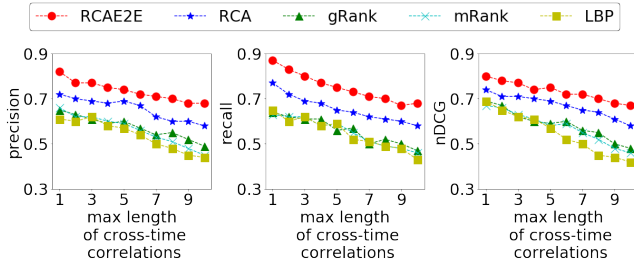


Figure 6: Performance vs. Max Length of Cross-Time Correlations

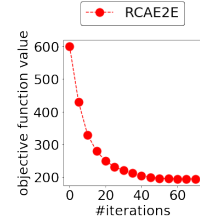


Figure 8: Convergence

data point will be the average of all \mathbf{s}^t corresponding to that data point.

5 Experiments

In the experimental part, we use synthetic data and real-world large-scale photoelectric factory data to verify the correctness and existence of our method hypothesis. We have chosen some state-of-the-art methods, including mRank and gRank [4], LBP [5], and RCA [1]. The methods we choose RCAE2E and other method parameters are BIC [12] and cross-validation. The evaluation metrics we used are precision, recall, and nDCG [13]. The precision, recall is calculated using the top- k results we found, and k is usually about two to three times the number of the true causal anomalies [5, 13]. The nDCG is calculated using the top- p results we found, and p is usually slightly smaller than the number of the true causal anomalies.

5.1 Synthetic Data

5.1.1 Data Generation There are two steps in data generation: generate the run data based on the synthetic profile, and add anomalies into the run data.

First, we will generate K MRFs, each of the MRF is generated based on Erdős-Rényi directed random graphs [14]. Then we will determine the cluster assignment of single run data. When we have MRFs and cluster assignments, we have the so-called synthetic profile. So we can generate the run data based on this synthetic profile. As for inserting anomalies into the data, we randomly select several nodes to make them the root cause anomalies, and then use Equation 4.12 to calculate the corresponding b . We use the amplitude-based anomaly generation method [1] to adjust the data to become anomalies by the value of b .

There are two parameters that are dynamic, which are the number of clusters (K) and the window size of multiple data points ($t-w$).

5.1.2 Performance vs. #states In Figure 5, we can clearly see the necessity of considering the diversity of states. This is because if they use only a single model to describe an end-to-end system with multiple states, the correlation network they created would not be able to describe the behavior of sensors in different states.

5.1.3 Performance vs. Max Length of Cross-Time Correlations In Figure 6, we can clearly see the necessity of separately considering the correlations with different time-lag. As the max length of cross-time

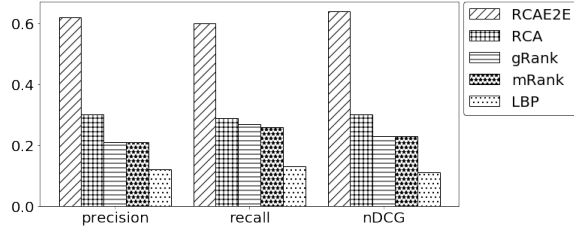


Figure 9: Performance

correlations increases, the performance of all methods will drop. But because RCAE2E separately considers the correlations with different time-lag, the performance does not drop as fast as other methods.

5.1.4 Noise Robustness In Figure 7, we can clearly see the necessity of considering Fault Propagation. The assumption of Fault Propagation is that the anomalies are noise if they won't propagate through the correlations. In other words, if we add noise to the data, the method of considering the Fault Propagation (RCA and RCAE2E) will not be affected too much.

5.1.5 Convergence In Figure 8, we can clearly see that every time we use Equation (4.15) to update the Problem (4.14), each update will monotonically decrease the value of the objective function.

5.2 Real-World Data

5.2.1 Data Description The real-world data we use here is the machine data of large photoelectric factory, and each machine contains hundreds of sensors. We have done some basic data preprocessing, such as screening data, filling in missing values, and standardizing data. In addition, we have aligned the data (all data should have both the same length of timestamp and the same name and quantity of sensors), and down-sampled the data. Finally, the data we fed to RCAE2E has the following data description: the number of run data is 136 ($R = 136$), the length of single run data is 1460 ($T = 1460$), and the number of sensors is 48 ($N = 48$).

5.2.2 Performance We have confirmed that there are multiple states in the data, so basically if the method does not take into account the diversity of the states, its performance will be very poor. In Figure 9, we can see that RCAE2E outperform other methods whether in precision, recall, or nDCG.

5.2.3 RCA + Different Clustering Methods RCA does not consider the diversity of the states, so

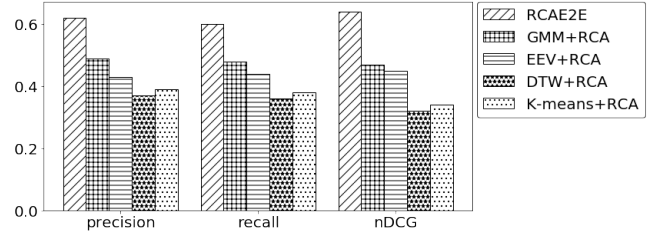


Figure 10: RCA + Different Clustering Methods

its performance will be very poor on data with multiple states. We combine RCA with some common clustering methods, and we can see that in Figure 10, their performances are indeed much better than the original RCA. But in Figure 10, we can see that RCAE2E still outperforms RCA with clustering.

6 Conclusion

In this paper, we present a framework called *Ranking Causal Anomalies in End-to-End System* (RCAE2E), which is a framework that can directly look for causal anomalies in the end-to-end system. Our contribution is that RCAE2E completely solve the problem of not considering the diversity of states and not separately considering the correlations with different time-lag in RCA. There are two main methods in RCAE2E, which are TICC_GTC and RCA_SCC. Finally, in the experimental part, we verify the correctness and existence of our method hypothesis.

References

- [1] Wei Cheng, Kai Zhang, Haifeng Chen, Guofei Jiang, Zhengzhang Chen, and Wei Wang. Ranking causal anomalies via temporal and dynamical analysis on vanishing correlations. In *Proceedings of the 22nd ACM SIGKDD International Conference on Knowledge Discovery and Data Mining*, pages 805–814. ACM, 2016.
- [2] J Gertler. Fault detection and diagnosis in engineering systems, 1998. *Maecel Dekker Inc., New York*, 1997.
- [3] Guofei Jiang, Haifeng Chen, and Kenji Yoshihira. Discovering likely invariants of distributed transaction systems for autonomic system management. In *Autonomic Computing, 2006. ICAC'06. IEEE International Conference on*, pages 199–208. IEEE, 2006.
- [4] Yong Ge, Guofei Jiang, Min Ding, and Hui Xiong. Ranking metric anomaly in invariant networks. *ACM Transactions on Knowledge Discovery from Data (TKDD)*, 8(2):8, 2014.
- [5] Changxia Tao, Yong Ge, Qinbao Song, Yuan Ge, and Olufemi A Omitaomu. Metric ranking of invariant networks with belief propagation. In *Data Mining (ICDM), 2014 IEEE International Conference on*, pages 1001–1006. IEEE, 2014.

- [6] David Hallac, Sagar Vare, Stephen Boyd, and Jure Leskovec. Toeplitz inverse covariance-based clustering of multivariate time series data. In *Proceedings of the 23rd ACM SIGKDD International Conference on Knowledge Discovery and Data Mining*, pages 215–223. ACM, 2017.
- [7] Denny Zhou, Olivier Bousquet, Thomas N Lal, Jason Weston, and Bernhard Schölkopf. Learning with local and global consistency. In *Advances in neural information processing systems*, pages 321–328, 2004.
- [8] Jerome Friedman, Trevor Hastie, and Robert Tibshirani. Sparse inverse covariance estimation with the graphical lasso. *Biostatistics*, 9(3):432–441, 2008.
- [9] Onureena Banerjee, Laurent El Ghaoui, and Alexandre d’Aspremont. Model selection through sparse maximum likelihood estimation for multivariate gaussian or binary data. *Journal of Machine learning research*, 9(Mar):485–516, 2008.
- [10] Robert M Gray et al. Toeplitz and circulant matrices: A review. *Foundations and Trends® in Communications and Information Theory*, 2(3):155–239, 2006.
- [11] Steffen L Lauritzen. *Graphical models*, volume 17. Clarendon Press, 1996.
- [12] Trevor Hastie, Robert Tibshirani, and Jerome Friedman. Unsupervised learning. In *The elements of statistical learning*, pages 485–585. Springer, 2009.
- [13] Kalervo Järvelin and Jaana Kekäläinen. Cumulated gain-based evaluation of ir techniques. *ACM Transactions on Information Systems (TOIS)*, 20(4):422–446, 2002.
- [14] Karthik Mohan, Palma London, Maryam Fazel, Daniela Witten, and Su-In Lee. Node-based learning of multiple gaussian graphical models. *The Journal of Machine Learning Research*, 15(1):445–488, 2014.